

Fig. 3. Electric shielding effectiveness at the center of rectangular cavity with multiple slots as a function of the number of slots;  $a = 1$  cm,  $T_a = 3a$ ,  $\alpha = 20$  cm,  $h = 50$  cm,  $d = 0.4$  cm,  $\theta = 0^\circ$ .

of the magnetic shielding effectiveness corresponds to ( $n = 1$ ,  $l = 2$ ) in the same equation.

Fig. 2 also shows that there is good agreement between the electric shielding effectiveness of the 2-D rectangular cavity with a slot and the measured one of the three-dimensional (3-D) rectangular cavity ( $40 \times 20 \times 50$  cm) with an aperture ( $10 \times 2$  cm) [6]. The reason of this good agreement is that the dominant electric field vector of the long and thin aperture on the 3-D rectangular cavity is perpendicular to the longer side of the aperture and is approximately uniform along the shorter side. This means that the dominant electric field of the aperture on the 3-D rectangular cavity is effectively equal to the electric field inside the slot of the 2-D rectangular cavity with TM-wave.

Fig. 3 shows the electric shielding effectiveness of the multiple slotted cavity ( $a = 1$  cm,  $T_a = 3a$ ,  $\alpha = 20$  cm,  $h = 50$  cm,  $d = 0.4$  cm, and  $\theta = 0^\circ$ ) at 100 and 600 MHz as varying the number of slots. Increasing the total area of slots by adding a slot one by one reduces the shielding effectiveness by about 3 dB each time.

#### IV. CONCLUSION

Electromagnetic wave penetration into 2-D multiple slotted rectangular cavity with TM-wave is investigated. By using the Fourier transform and the mode-matching technique, we obtain a solution in a fast-converging series form. Numerical computations are accomplished to show the shielding effectiveness inside the cavity in terms of the size of the cavity and the slot and the number of slots.

#### REFERENCES

- [1] E. Arvas and T. K. Sarkar, "TM transmission through dielectric-filled slots in a conducting cylindrical shell of arbitrary cross section," *IEEE Trans. Electromagn. Compat.*, vol. EMC-29, pp. 150–156, May 1987.
- [2] L. K. Wu and L. T. Han, "E-polarized scattering from a conducting rectangular cylinder with an infinite axial slot filled by a resistively coated dielectric strip," *IEEE Trans. Antennas Propagat.*, vol. 40, pp. 731–733, June 1992.
- [3] J. V. Tejedor, L. Nuno, and M. F. Bataller, "Susceptibility analysis of arbitrarily shaped 2-D slotted screen using a hybrid generalized matrix finite-element technique," *IEEE Trans. Electromagn. Compat.*, vol. 40, pp. 47–54, Feb. 1998.
- [4] T. M. Wang, A. Cuevas, and H. Ling, "RCS of a partially open rectangular box in the resonant region," *IEEE Trans. Antennas Propagat.*, vol. 38, pp. 1498–1504, Sept. 1990.

- [5] H. H. Park and H. J. Eom, "Electrostatic potential distribution through thick multiple rectangular apertures," *Electron. Lett.*, vol. 34, no. 15, pp. 1500–1501, July 1998.
- [6] B. W. Kim, Y. C. Chung, and T. W. Kang, "Analysis of electromagnetic penetration through apertures of shielded enclosure using finite element method," in *14th Annu. Rev. Progress Appl. Computat. Electromagn.*, vol. II, Mar. 1998, pp. 795–798.

## High-Gain Low-Sidelobe Double-Vee Dipoles

Neal Patwari and Ahmad Safaai-Jazi

**Abstract**—This paper introduces a novel variation of the vee dipole antenna consisting of two coplanar vee dipoles with a common feed point. It is referred to as a *double-vee dipole*. Radiation characteristics of the double-vee dipole antenna are investigated numerically and experimentally. It is shown that the double-vee dipole can provide significantly higher directivity and lower sidelobes and back radiation than the conventional vee dipole. With increasing arm length, the directivity of the double-vee dipole exhibits a series of local maxima. Measured and predicted radiation patterns for a fabricated double-vee dipole are presented and shown to be in good agreement.

**Index Terms**—Dipole antennas, directive wire antennas, vee antenna.

#### I. INTRODUCTION

The vee dipole is a well-known geometry developed as a modification to the linear dipole with the aim of increasing its directivity [1]. It has also been shown that by using an arm-shaping technique involving parabolic shapes, the directivity of dipoles can be increased [2]. Double-vee dipole configurations have been investigated for the generation of circularly polarized fields [3]. In such antennas, the vee dipoles have separate feed points and lie in different planes. The double-vee dipole presented here consists of two coplanar vee dipoles with a common feed point. Numerically calculated radiation characteristics and measured far-field radiation patterns are presented in this paper and show that the double-vee dipole can increase directivity and decrease sidelobe level and back radiation compared to the vee dipole. The measurement of the radiation pattern of one double-vee dipole is detailed in this article as a representative case.

#### II. DESIGN OPTIMIZATION

A double-vee dipole is specified using four independent geometrical parameters, as shown in Fig. 1. The simulation uses the Numerical Electromagnetics Code v.2 (NEC-2) to perform an exhaustive optimization search. Each possible geometry (with a length granularity of  $0.03\lambda$  and a angle granularity of  $1^\circ$ ) over wide ranges of all four parameters is simulated. The exterior arm length is varied over a range of  $1.0\lambda < L_1 < 3.0\lambda$ , while the interior arm is kept shorter than exterior arm to limit the footprint:  $0 < L_2 < L_1$ . The angle of the exterior arm is varied over a range of  $3^\circ < \Psi_1 < 90^\circ$ , while the interior arm angle  $\Psi_2$  is always at least  $3^\circ$  smaller than  $\Psi_1$ . Allowing

Manuscript received October 30, 1998; revised September 15, 1999. This work was supported by a National Science Foundation Graduate Fellowship. N. Patwari is with Motorola Labs, Plantation, FL 33322 USA. A. Safaai-Jazi is with the Bradley Department of Electrical and Computer Engineering, Virginia Tech, Blacksburg, VA 24061-0111 USA. Publisher Item Identifier S 0018-926X(00)01657-4.

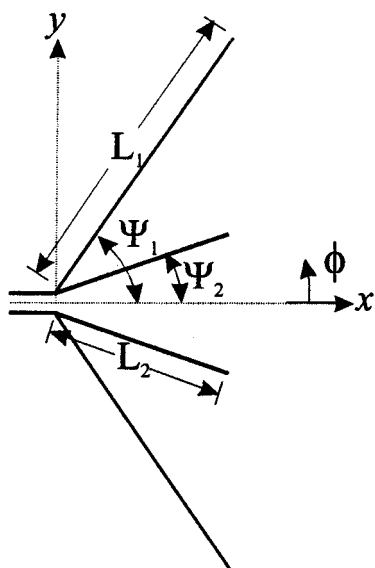


Fig. 1. Geometry and coordinates for the double-vee dipole.

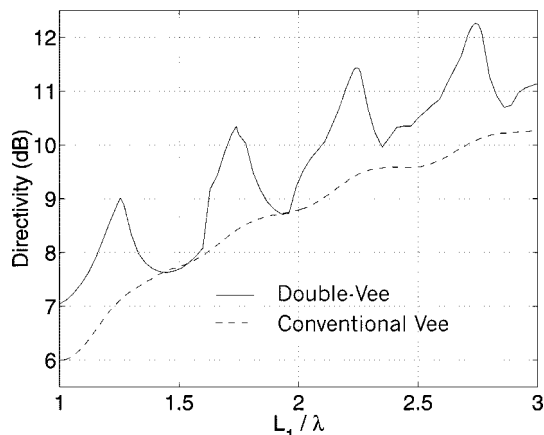


Fig. 2. Variations in maximum directivity versus  $L_1/\lambda$  for conventional and double-vee dipoles.

the arm wires to be closer than  $3^\circ$  to each other would make the antenna difficult to fabricate and also lead to numerical inaccuracies in NEC-2 simulation results.

After tabulating all of the simulation results, geometries are found that produce the highest directivity for each exterior arm length  $L_1$ . In Fig. 2, this directivity is plotted. Also plotted, for comparison, is the NEC-2 predicted directivity of a conventional vee dipole with length  $L_1$  and the optimum angle given in [1].

### III. RADIATION CHARACTERISTICS

The results in Fig. 2 show that the directivity of the double-vee dipole can be as much as 2.2 dB higher than the conventional vee dipole with the same arm length. It is further observed that as a function of  $L_1$ , the directivity of the double-vee dipole exhibits a series of local maxima. The geometries of the double-vee dipoles corresponding to the four local maxima in Fig. 2 are referred to here as the *optimum solutions* and are described in Table I. An antenna designer should use these geometrical parameters to take full advantage of the higher directivity and lower sidelobe and backlobe radiation levels that are possible with the double-vee dipole.

The average front-to-back ratio for the four optimum solutions listed in Table I is 10 dB. For the smallest optimum solutions (#1 and #2), the

TABLE I  
OPTIMUM-DIRECTIVITY DOUBLE-VEE DIPOLE SOLUTIONS: DESIGN  
PARAMETERS AND CHARACTERISTICS

Parameters	Solution 1	Solution 2	Solution 3	Solution 4
$L_1$	$1.255\lambda$	$1.745\lambda$	$2.245\lambda$	$2.740\lambda$
$L_2$	$0.855\lambda$	$1.355\lambda$	$1.855\lambda$	$2.355\lambda$
$\Psi_1$	$53^\circ$	$44^\circ$	$38^\circ$	$35^\circ$
$\Psi_2$	$41^\circ$	$29^\circ$	$25^\circ$	$23^\circ$
Directivity	8.0	10.8	13.9	16.8
3dB Beamwidth	$24^\circ$	$20^\circ$	$18^\circ$	$16^\circ$
Max Sidelobe Level	-8.6 dB	-9.0 dB	-10.3 dB	-9.3 dB
Front/Back Ratio	11.9 dB	10.1 dB	10.3 dB	9.3 dB
3dB Bandwidth	11.0%	7.2%	5.8%	4.7%
Input Resistance	$341\Omega$	$388\Omega$	$386\Omega$	$395\Omega$
Input Reactance	$163\Omega$	$110\Omega$	$106\Omega$	$98\Omega$

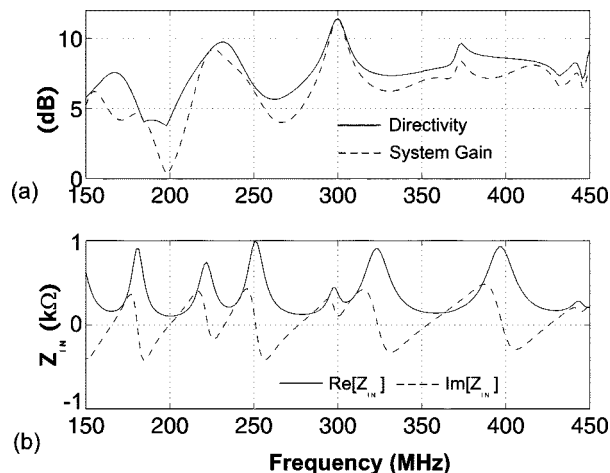


Fig. 3. (a) Directivity, antenna system gain (directivity minus reflection loss). (b) Input impedance versus frequency for optimum solution #3 designed for  $f_c = 300$  MHz.

backlobe is lower than the other sidelobes. With each larger optimum solution, the backlobe radiation level increases while the other sidelobe levels decrease. Overall, the beamwidth decreases and the directivity increases, even as the front-to-back ratio decreases. The backlobe radiation level of the double-vee dipole is about 7 dB lower than that of a conventional vee dipole [1]. It is particularly interesting that the optimum solutions have  $L_1$  and  $L_2$  that increment by approximately  $\lambda/2$  for each larger solution. It can be inferred from these results that even larger, more directive optimum solutions can be found by successively raising  $L_1$  and  $L_2$  by  $\lambda/2$  and then finding the optimum  $\Psi_1$  and  $\Psi_2$ . The input impedance has a significant reactive component that arises from the resonant nature of the double-vee dipole. The real and imaginary parts of the input impedance are about 400 and  $100\Omega$ , respectively, at the center frequencies of optimum solutions two, three, and four. Fig. 3(b) shows the input impedance of a double-vee dipole designed for optimum solution #3 at a center frequency  $f_c = 300$  MHz. To show the effects of the input impedance on the bandwidth, the an-

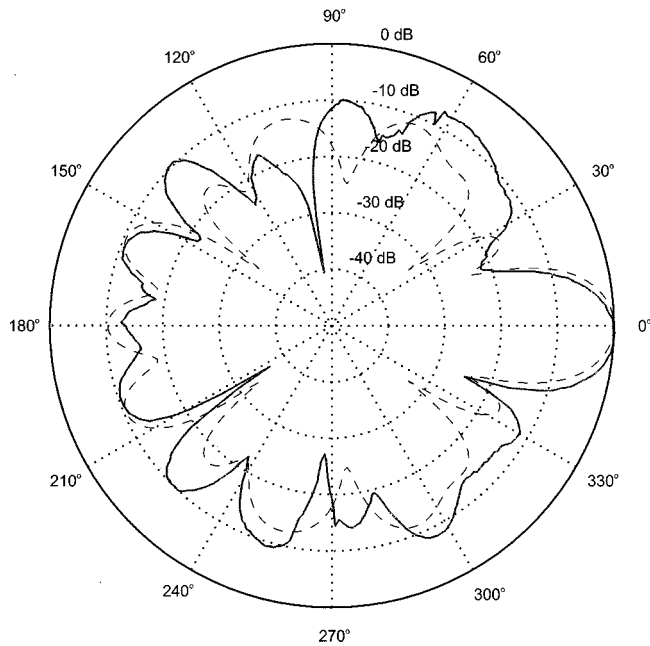


Fig. 4. Predicted (---) and measured (—) E-plane radiation pattern, optimum solution #3 with parameters given in Table I with  $\lambda = 12.5$  cm.

tenna is matched to a  $300\Omega$  transmission line by means of a short-circuit single-stub tuner. The tuner is arranged such that the double-vee dipole is perfectly matched to  $300\Omega$  at the antenna's center frequency. Fig. 3(a) plots the directivity of the antenna and the antenna system gain (the directivity minus the reflection loss) versus frequency. The 3-dB bandwidth of each optimum solution double-vee dipole, assuming that a short-circuit single-stub tuner is used for perfect matching at  $f_c$  is given in Table I. Note from Fig. 3(a) that a double-vee dipole designed for maximum directivity at 300 MHz can also be operated at other frequencies. Different multiband characteristics are possible with each optimum solution.

Measurements of all four optimum solution double-vee dipoles were conducted. Each was constructed using aluminum wire with a diameter of 3 mm and mounted on thin cardboard. The double-vee dipole at the optimum solution #1 was constructed with  $\lambda = 20$  cm and measured at 1.5 GHz and was presented in the preliminary phase of our research [4]. The other three double-vee dipoles were built with  $\lambda = 12.5$  cm and measured at 2.4 GHz. Fig. 4 shows the measured far-field E-plane pattern in decibels for optimum solution #3. The measured and predicted half-power beamwidths are the same at  $18^\circ$ . The measured back radiation level is more than 10 dB below the main lobe peak. Also shown in Fig. 4 are the numerically calculated radiation patterns from NEC-2. The measured and predicted patterns for all four optimum solutions show similar agreement.

#### IV. CONCLUSIONS

The double-vee dipole is as compact and low-cost as the vee dipole but has significant advantages. In this paper, a series of optimum solutions for the double-vee dipole are presented that yield sidelobe and backlobe radiation level reductions of up to 7 dB and directivity increases of 2.2 dB compared to the vee dipole. The double-vee dipole is also shown to be well suited for multiband operation. Radiation properties of the optimum solutions are investigated both numerically and experimentally. Since measured results accurately match numerical results, the double-vee dipole promises simple and predictable design

and construction. The calculated and measured results both suggest that the double-vee dipole is a promising candidate for applications, where the bandwidth requirement is modest and higher gain and lower side-lobe and backlobe levels are desired to reduce interference effects and, hence, improve the quality of information signals.

#### ACKNOWLEDGMENT

The authors would like to thank M. Barts and R. Neely of the Virginia Tech Antenna Laboratory for the measurements.

#### REFERENCES

- [1] G. A. Thiele and E. P. Ekelman, "Design formulas for vee dipoles," *IEEE Trans. Antennas Propagat.*, vol. AP-28, pp. 588–590, July 1980.
- [2] D. K. Cheng and C. H. Liang, "Shaped wire antennas with maximum directivity," *Electron. Lett.*, vol. 18, Sept. 16, 1982.
- [3] H.-W. Tseng and B. A. Munk, "The generation of omnidirectional circularly polarized far field by a pair of orthogonally oriented vee dipoles," in *AP-S Int. Symp.*, vol. 2, Ann Arbor, MI, July 1993, pp. 1042–1045.
- [4] H. Patwari and A. Safaai-Jazi, "Predictions and measurements of double-vee dipoles," in *AP-S Int. Symp.*, vol. 3, Atlanta, GA, June 1998, pp. 1426–1429.
- [5] W. L. Stutzman and G. A. Thiele, *Antenna Theory and Design*, 2nd ed. New York: Wiley, 1998.

### Exact Geometrical Optics Solution for an Isorefractive Wedge Structure

Piergiorgio L. E. Uslenghi

**Abstract**—A structure consisting of four right-angle wedges with a common edge, made of four different materials isorefractive to one another is considered. If a certain relation is satisfied among the four intrinsic impedances of the materials, then an incident plane wave generates reflected and transmitted plane waves that constitute the exact solution to the boundary-value problem. This geometrical-optics exact solution is valid for arbitrary polarization and arbitrary direction of incidence of the primary wave.

**Index Terms**—Complex media, electromagnetic diffraction, electromagnetic reflection and transmission, geometrical optics, isorefractive material.

#### I. INTRODUCTION

Boundary-value problems involving isorefractive materials and for which geometrical optics represents the exact solution have been solved for a wedge structure [1] and a paraboloid [2] under plane wave excitation and for an isolated wedge with a line source at its edge [3]. In this letter, a new solution is presented for a structure consisting of four  $90^\circ$  wedges with a common edge, each filled with a linear, homogeneous, and isotropic material. The four materials are isorefractive to one another. It is shown that geometrical optics yields the exact solution when the primary source is a plane wave with arbitrary direction of incidence and arbitrary polarization, provided that a certain relation is satisfied among the intrinsic impedances of the four materials. This new solution was presented recently at a symposium [4].

Manuscript received October 20, 1998; revised October 26, 1999.

The author is with the Department of Electrical Engineering and Computer Science, University of Illinois at Chicago, Chicago, IL 60607-7053 USA.

Publisher Item Identifier S 0018-926X(00)01659-8.